

Influence-Based Reward Modulation for Implicit Communication in Human-Robot Interaction

Haoyang Jiang¹, Elizabeth A. Croft², Michael G. Burke¹

¹Monash University, Melbourne, Australia

²University of Victoria, Victoria, Canada

haoyang.jiang@monash.edu, ecroft@uvic.ca, michael.g.burke@monash.edu

Abstract—Communication is essential for successful interaction. In human-robot interaction, implicit communication holds the potential to enhance robots’ understanding of human needs, emotions, and intentions. This paper introduces a method to foster implicit communication in HRI without explicitly modelling human intentions or relying on pre-existing knowledge. Leveraging Transfer Entropy, we modulate influence between agents in social interactions in scenarios involving either collaboration or competition. By integrating influence into agents’ rewards within a partially observable Markov decision process, we demonstrate that boosting influence enhances collaboration, while resisting influence diminishes performance. Our findings are validated through simulations and real-world experiments with human participants in social navigation settings.

I. INTRODUCTION

It is widely recognised that communication is key to successful interaction. Humans communicate with each other through both explicit (direct, deliberate communication over an established channel with clear intent to reach a defined recipient [1]) and implicit channels. Implicit communication is a subtle, indirect mode of conveying information, often relying on context, nonverbal cues, and shared understanding between communicators to convey meaning without explicit verbalisation [2]. Implicit communication is particularly crucial for human-robot interaction as it enhances a robot’s ability to proactively understand and respond to human needs, emotions, and intentions, thereby facilitating more natural and effective communication and collaboration between humans and robots. To date, most current human-robot interaction (HRI) studies focusing on implicit communication explicitly model the intention of human participants [3] [4], or rely on existing intention knowledge [5]. This information is challenging to obtain in general settings.

This paper proposes a method to facilitate implicit communication without the need to explicitly model human participants or rely on pre-existing knowledge. Our approach conceptualises communication as the degree of influence agents have on one another, employing information-theoretic techniques. Specifically, we use Transfer Entropy (TE) [6], a measure of directed information transfer, to modulate influence in social interactions. We illustrate our method using a social navigation setting [7], targeting scenarios where the objectives of individual agents may result in a need for either collaboration or competition. In particular, we demonstrate the proposed method in a *corridor dilemma* setting, a popular

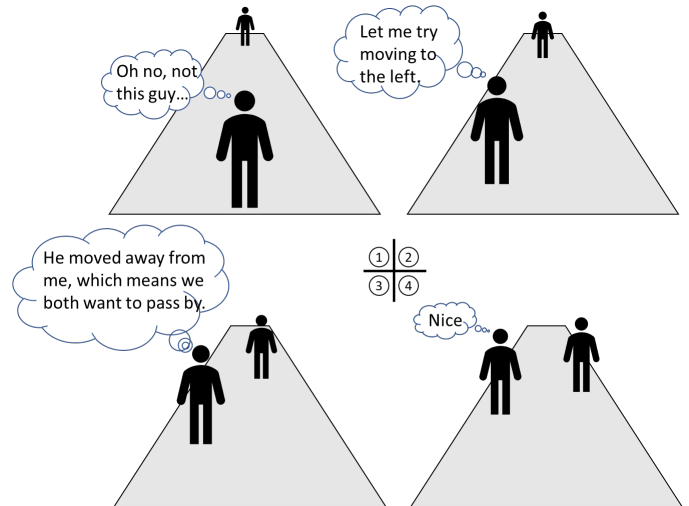


Fig. 1: Humans rely on implicit communication and information exchange to negotiate complex social settings. This work introduces a reward augmentation framework to emulate this implicit communication behaviour. We show that by optimising robot policies to increase information flow, we can influence human behaviour and improve human-robot collaboration.

scenario in HRI [8] [9]. For our experiments, we define this as a scenario where individuals encounter each other in a narrow passage and where a given agent may wish to meet or avoid another agent (Figure 1). This scenario involves implicit information exchange, where participants attempt to discern each other’s intentions without verbal communication. By observing and reacting to subtle cues such as changes in trajectories, participants estimate each other’s objectives to inform their own actions. Interactions of this form can be complex, especially when both participants act simultaneously, leading to a state of “resonance” that dissipates as mutual understanding is achieved.

To better equip robots with the ability to handle this type of setting, we consider a partially observable Markov decision process (POMDP) and propose a novel approach that augments the rewards of agents to include the TE that boosts or resists influence between agents. We find that boosting influence enhances the other participant’s ability to collaborate or compete

with the ego-agent, while resisting influence mainly diminishes their ability to collaborate. These findings hold both in self-play [10] simulations and in virtual human-agent experiments. Real-world human-robot experiments with physical robots also show that boosting influence improved collaboration, but reduced competition performance. Overall, our work makes the following contributions and findings:

- We propose a novel framework for enhancing implicit communication in social HRI through influence modulation, without requiring explicit modelling or prior knowledge of humans.
- We evaluate the framework in both simulation and virtual human-agent interaction environments, finding that promoting information transfer promotes collaboration and benefits the human in competitive scenarios.
- We show that this collaborative effect holds in real-world human-robot experiments, but reveal interesting discrepancies in competitive interactions.

II. RELATED WORK

Implicit communication has attracted significant attention in the field of robotics. Che et al. [3] present a planning framework that integrates implicit and explicit communication during mobile robot navigation, using a human behaviour model and inverse reinforcement learning to generate communicative actions that enhance robot transparency and efficiency. Li and Zhang [11] [12] introduce a novel interaction framework that enables communication between humans and assistive devices, leveraging gaze movements to infer human intent. Liang et al. [13] investigate the role of implicature, a form of implicit communication, in HRI using the cooperative card game Hanabi, to demonstrate that human players paired with an implicature AI are significantly more likely to perceive their partner as human. These implicit communication studies typically involve explicit modelling of other participants or rely on pre-existing social knowledge [5]. In contrast, our approach is model-free, and does not require pre-existing social knowledge.

Implicit communication is closely related to intent communication, which aims to allow observers to easily deduce the intent behind generated behaviours [14] [15]. Motions conveying intent have been shown to enhance perceived safety in virtual human-robot path-crossing tasks [16]. In reinforcement learning settings, robustness, efficiency and energy reward terms have been shown to enhance the ability of humans to interpret a robot’s intent [14]. Research focusing on projected visual legibility cues [17] has indicated that projected arrows generally offer greater interpretability than flashing lights in navigation settings. Notably, the means through which people convey and comprehend intent vary, and there exists no universally applicable method for assessing intent communication. By viewing communication as the exchange of information between agents, our TE-based framework holds the potential to adapt to various forms of communication, offering a versatile method to shape communication dynamics. Importantly, unlike many of the uni-directional intent communication approaches

above, our framework captures the multi-directional nature of communication.

Transfer Entropy (TE) is a mathematical concept introduced by Schreiber [6] that quantifies the directional flow of information between two random processes. Formally, TE is defined as the difference between the conditional entropies of one process given the past of another and the past of itself. This is expressed mathematically as

$$TE(X \rightarrow Y) = H(Y_t|Y_{t-1}, Y_{t-2}, \dots) - H(Y_t|Y_{t-1}, Y_{t-2}, \dots, X_{t-1}, X_{t-2}, \dots), \quad (1)$$

where H denotes entropy, and X and Y are the two stochastic processes under consideration. By measuring how much uncertainty about the future state of one process is reduced when the past of another process is known, TE provides a rigorous framework for assessing information transfer. This ability to capture not just correlations but also the causal influence between processes makes TE particularly useful for analysing complex interactions in diverse fields such as neuroscience, economics, and human behaviour, where understanding the directionality of information flow is crucial. TE is most prevalent in economics literature [18, 19], but has also been used to analyse animal-animal or animal-robot interactions [20][21], joint attention [22] and to model pedestrian evacuation [23]. Berger et al. [24] apply TE to detect human-to-robot perturbations using low-cost sensors. TE has also been used to identify arbitrary cues from raw social interaction data between humans [25]. These works successfully quantify information transfer or the relationship between sources of information, but tend to focus on specific features or aspects of interest. Our work seeks to extend the use of TE to provide a more general approach aimed at enhancing information transfer in decision-making settings, leading to improved human-robot collaboration. Our core assumption is that greater transparency or information transfer reduces information asymmetry [26], thereby enhancing collaboration potential. In this paper we leverage TE to control information asymmetry, and tip the balance of power in favour of or against opponents.

Social learning: Mutual information (MI) is an information measure that captures the shared information between random variables, which has been widely used for social learning. Klyubin et al. [27] proposed the concept of empowerment for intrinsic motivation for reinforcement learning, which measures the maximum MI (channel capacity) between an agent’s actuators and their sensors. This concept was expanded by Mohamed and Rezende with a lower complexity maximisation approach to MI [28]. Jaques et al. use MI as a social influence reward for multi-agent deep reinforcement learning in Sequential Social Dilemmas (SSDs) [29] to encourage collaborations between agents [30]. While MI measures the shared information between random variables, TE measures the time-asymmetric information transfer. Unlike MI, the asymmetric nature of TE enables us to capture the directionality of information flow, which is advantageous for social

communication. By leveraging TE, our goal is to quantify and modulate social information transfer.

III. METHODOLOGY

We consider an environment with multiple agents, each possessing distinct states, actions, and rewards. These rewards can be complementary (collaborative), competitive, or unrelated. The ego-agent aims to maximise its own rewards, ideally without negatively impacting other agents. In a HRI context, we posit that the robot should exhibit behaviour perceived as altruism. A fair outcome involves promoting collaboration, yielding to humans in competitive scenarios, and allowing independent agents to achieve their objectives if there is no conflict of interest. Within this environment, the ego-agent has complete access to its own state and can observe other agents, but may lack access to their decision-making processes or complete states. Consequently, we model interaction as a partially observable Markov decision process (POMDP), where states represent system situations and actions determine transitions between these states. Observations derived from states guide decision-making despite incomplete information.

The core concept behind the proposed method involves leveraging influence as an additional reward to enhance implicit communication between agents. This augmentation aims to accelerate learning and ultimately improve the collaboration performance for all agents or competitive capability of the other agents. Below, we assume two agents, labelled as $P1$ and $P2$ with $P1$ the ego-agent. By computing the TE from the historical actions of $P2$ (other agent) to the current action of $P1$ (ego-agent), $P1$ can better respond to $P2$ without an explicit model. This TE is computed as $TE_{\mathbf{a}_{2,t}^{(n)} \rightarrow a_{1,t}}$, where $a_{1,t}$ is ego-agent's action at time t , $\mathbf{a}_{2,t}^{(n)} = (a_{2,t-1}, a_{2,t-2}, \dots, a_{2,t-n})$ comprises historical actions of $P2$, and n is the history length. We augment the TE into the reward function,

$$\text{Reward}_{a_{1,t}} = \phi TE_{\mathbf{a}_{2,t}^{(n)} \rightarrow a_{1,t}} + r. \quad (2)$$

Here r is the reward related to the agent's objectives and ϕ is a scaling factor used to adjust the strength of the TE reward. Importantly, augmenting the reward with this TE implies encouraging the ego-agent to take actions that promote influence from past actions of the other agent to the current action of the ego-agent, making it more legible [15] to other agents. This occurs because of the ego-agent's clearer response to the other agent's actions, allowing us to affect other agents without requiring access to their behaviour models.

A. Measuring influence

We manipulate the influence using the Transfer Entropy, $T_{Y \rightarrow X}$, between the time series of state and action pairs. Transfer entropy is closely related to *Wiener-Granger causality* [31], and computes the conditional mutual information between two variables X_t and Y_t [32],

$$\begin{aligned} T_{Y \rightarrow X}^{(k,l)}(t) &= I(X_t : \mathbf{Y}_t^{(l)} | \mathbf{X}_t^{(k)}) \\ &= H(X_t | \mathbf{X}_t^{(k)}) - H(X_t | \mathbf{X}_t^{(k)}, \mathbf{Y}_t^{(l)}). \end{aligned} \quad (3)$$

Here, I denotes mutual information, while H represents Shannon's entropy [33]. This equation measures the directed transfer of information from Y to X , with t indicating time. The terms $\mathbf{Y}_t^{(l)}$ and $\mathbf{X}_t^{(k)}$ denote sequences of past observations for Y and X , respectively, with lengths k and l ,

$$\begin{aligned} \mathbf{X}_t^{(k)} &= (x(t-\delta), x(t-2\delta), \dots, x(t-(k-1)\delta)) \\ \mathbf{Y}_t^{(l)} &= (y(t-\delta), y(t-2\delta), \dots, y(t-(l-1)\delta)). \end{aligned} \quad (4)$$

Here δ is the unit time step. In literature, X is referred to as the 'target' and Y as the 'source'. Transfer entropy can be intuitively understood as the decrease in uncertainty within a state X , predicted solely based on its own past, upon the introduction of an additional information source Y [32].

In order to compute TE, we calculate two entropy terms, the first assumes that there is influence from past actions of the other agent $P2$ to the current action of the ego-agent $P1$ (superscript $+$), while the second assumes no influence (superscript $-$). We denote $\mathbf{s}_{1,t}^{(n)} = (s_{1,t}, s_{1,t-1}, s_{1,t-2}, \dots, s_{1,t-n})$ and $\mathbf{o}_{2,t}^{(n)} = (o_{2,t}, o_{2,t-1}, o_{2,t-2}, \dots, o_{2,t-n})$, where $s_{1,t}, s_{1,t-1}, \dots, s_{1,t-n}$ and $o_{2,t}, o_{2,t-1}, \dots, o_{2,t-n}$ comprise the states of the ego-agent $P1$ and observations of agent $P2$ at time $t, t-1, \dots, t-n$ respectively. We then compute probability distributions over the actions (policies) for each of these scenarios:

$$\begin{aligned} P_{a_{1,t}}^+ &= P(a_{1,t} | \mathbf{s}_{1,t}^{(n)}, \mathbf{o}_{2,t}^{(n)}), \\ P_{a_{1,t}}^- &= P(a_{1,t} | \mathbf{s}_{1,t}^{(n)}) \end{aligned} \quad (5)$$

and calculate Shannon's entropy. Here we show the formulation for discrete Shannon's entropy, but Shannon's differential entropy should be used if the action space is continuous. We can now calculate the TE, or information flowing from past actions of $P2$ to the current action of $P1$.

$$\begin{aligned} TE_{\mathbf{a}_{2,t}^{(n)} \rightarrow a_{1,t}} &= TE_{f(\mathbf{o}_{2,t}^{(n)}) \rightarrow a_{1,t}} = H(P_{a_{1,t}}^-) - H(P_{a_{1,t}}^+) \\ &= \left[- \sum_{p \in P_{a_{1,t}}^-} p(a_{1,t} | \mathbf{s}_{1,t}^{(n)}) \log_2 p(a_{1,t} | \mathbf{s}_{1,t}^{(n)}) \right] \\ &\quad - \left[- \sum_{p \in P_{a_{1,t}}^+} p(a_{1,t} | \mathbf{s}_{1,t}^{(n)}, \mathbf{o}_{2,t}^{(n)}) \log_2 p(a_{1,t} | \mathbf{s}_{1,t}^{(n)}, \mathbf{o}_{2,t}^{(n)}) \right]. \end{aligned} \quad (6)$$

Our hypothesis is that manipulating TE will allow us to control the influence during social interactions. For instance, taking actions to increase TE could promote influence, which could sequentially enhance collaboration between agents. Ideally, being responsive and legible would aid all participants to achieve their goals during interactions. However, this strategy may become self-sacrificing or altruistic in some settings, a phenomena often explored in game theory [34]. This happens when being legible conflicts with an agent's primary goal, or when an interaction is competitive.

Entropy measures the degree of uncertainty in actions: higher entropy means greater uncertainty, and lower entropy means less. Increasing $TE_{\mathbf{a}_{2,t}^{(n)} \rightarrow a_{1,t}}$ increases the uncertainty of actions when ignoring other agents and decreases the uncertainty when considering them (i.e., $H(P_{a_{1,t}}^-)$ and $H(P_{a_{1,t}}^+)$)

in Equation (6) respectively), thus promoting influence. Conversely, decreasing TE resists this influence.

B. Q-learning

The TE calculations above require distributions over actions (a policy). We illustrate how these can be obtained using Q-learning [35]. However, it is important to highlight that our approach is not restricted to Q-learning and could be used with other probabilistic policies obtained through reinforcement learning. We employ Temporal Difference learning [36] to find Q-values representing the expected cumulative rewards for actions in specific states, following the Bellman equation [37],

$$Q(s, a) \leftarrow (1 - \alpha)Q(s, a) + \alpha(r + \gamma \max_{a'} Q(s', a')). \quad (7)$$

Here $Q(s, a)$ is the Q-value for state s and action a , α is the learning rate, r is the immediate reward, γ is the discount factor, s' is the next state and a' is the action in the next state. This iterative process enables the agent to learn the optimal Q-values over time, determining the most advantageous actions to take in various states. The optimal action a^* at current state is determined by

$$a^* = \operatorname{argmax}_a Q(s, a). \quad (8)$$

In contrast to this deterministic policy, a probabilistic policy can be employed by converting the Q values to probabilities, then sampling from the distribution to choose the action. We do this by taking the softmax [38] over Q-values at a given state.

$$a^* \sim P_a = \operatorname{Softmax}(Q(s, a)|_s) \quad (9)$$

Q-learning often uses an epsilon-greedy strategy [39] to balance exploration and exploitation. This approach alternates between choosing actions with the highest Q-value and occasionally exploring other options with a small probability (ϵ). We use this strategy in our implementations.

In the proposed multi-agent setting where states are not fully observable, s in Q-learning (referring to $Q(s, a)$) becomes the states of ego-agent and observations of other agents' states in the scene. To be specific, s comprises $\mathbf{s}_{1,t}^{(n)}$ and $\mathbf{o}_{2,t}^{(n)}$, which denote the states of $P1$ and observations of $P2$ at time $t, t-1, \dots, t-n$ respectively. The action a is simply the actions of the agent $P1$ at time t (i.e., $a_{1,t}$), resulting in the expanded Q table,

$$Q(s, a) = Q(a_{1,t}, \mathbf{s}_{1,t}^{(n)}, \mathbf{o}_{2,t}^{(n)}), \quad (10)$$

and probabilistic Q-learning policy

$$a_{1,t}^* \sim P_{a_{1,t}} = \operatorname{Softmax}(Q(a_{1,t}|\mathbf{s}_{1,t}^{(n)}, \mathbf{o}_{2,t}^{(n)})). \quad (11)$$

This distribution over actions allows us to compute TE using the Q table. First, for the entropy assuming influence, we can directly use the original Q table from Equation (11) as the probability distribution over actions:

$$P_{a_{1,t}}^+ = \operatorname{Softmax}(Q(a_{1,t}|\mathbf{s}_{1,t}^{(n)}, \mathbf{o}_{2,t}^{(n)})). \quad (12)$$

In order to measure the entropy assuming no influence, the other agent's ($P2$'s) history in the Q table can be marginalised over:

$$Q(a_{1,t}, \mathbf{s}_{1,t}^{(n)}) = \frac{1}{m} \sum_{\mathbf{o}_{2,t}^{(n)}} Q(a_{1,t}, \mathbf{s}_{1,t}^{(n)}, \mathbf{o}_{2,t}^{(n)}), \quad (13)$$

with m the number of possible observations $\mathbf{o}_{2,t}^{(n)}$. Then the same process as above is repeated to compute the action distributions assuming no influence:

$$P_{a_{1,t}}^- = \operatorname{Softmax}(Q(a_{1,t}|\mathbf{s}_{1,t}^{(n)})). \quad (14)$$

We can now calculate the TE according to Equation (6) and incorporate this into the reward term in the POMDP according to Equation (2).

C. Connections to Legibility

The proposed TE augmentation is closely related to legibility. Dragan et al. [15] formalise legible motion as motion that enables an observer to confidently infer the correct goal configuration after observing only a snippet of the trajectory. To do so, they propose a metric to evaluate legibility in a trajectory planning scenario, with the legibility $L(\xi)$ of a trajectory ξ defined as:

$$L(\xi) = \frac{\int P(G^*|\xi)f(t)dt}{\int f(t)dt},$$

where G^* is the actual goal across the trajectory. Trajectories are more legible if the probability $P(G^*|\xi)$ is higher. Consider an interactive scenario with two agents, agent 1 and agent 2. Denoting the trajectory or action of agent 1 by τ_1 and agent 2 by τ_2 , and their goals g_1 and g_2 , the legibility of agent 2 from the perspective of agent 1 can be expressed as:

$$L(g_2|\tau_2, \tau_1) = P(g_2|\tau_2, \tau_1).$$

Using Bayes theorem, this probability can be expressed as:

$$P(g_2|\tau_2, \tau_1) = \frac{P(\tau_2|g_2, \tau_1)P(g_2|\tau_1)}{P(\tau_2|\tau_1)}.$$

Now consider the TE from agent 1's trajectory to agent 2's trajectory, and for simplification, let us assume a history length of 1:

$$\begin{aligned} TE(\tau_1 \rightarrow \tau_2) &= H(\tau_2(t)|\tau_2(t-1)) \\ &\quad - H(\tau_2(t)|\tau_2(t-1), \tau_1(t-1)) \\ &= P(\tau_2(t), \tau_2(t-1), \tau_1(t-1)) \\ &\quad \log \left[\frac{P(\tau_2(t)|\tau_2(t-1), \tau_1(t-1))}{P(\tau_2(t), \tau_2(t-1))} \right]. \end{aligned} \quad (15)$$

This measures the amount of information that the past states of agent 1 ($\tau_1(t-1)$) provide about the future states of agent 2 ($\tau_2(t)$), over and above the information provided by the past states of agent 2 ($\tau_2(t-1)$) alone. The term

$$\log \frac{P(\tau_2(t)|\tau_2(t-1), \tau_1(t-1))}{P(\tau_2(t), \tau_2(t-1))}$$

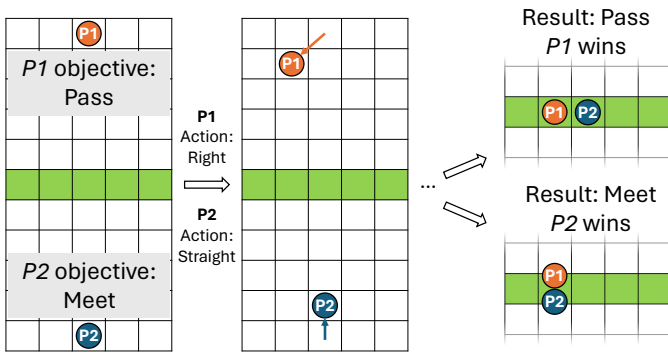


Fig. 2: A corridor dilemma episode: $P1$ is assigned to pass, and $P2$ is assigned to meet. In the first turn, $P1$ chose *right*, and $P2$ chose *straight*. After 5 turns, the result could be either *pass* (as in the top scenario), making $P1$ the winner, or *meet* (as in the bottom scenario), making $P2$ the winner.

captures how much additional information about $\tau_2(t)$ is provided by $\tau_1(t-1)$ over and above $\tau_2(t-1)$. TE extends mutual information to consider the temporal dynamics and causality between the time series [6]. Thus, TE also includes mutual information about how τ_1 affects τ_2 . This affects both $P(\tau_2|g_2, \tau_1)$ and $P(\tau_2|\tau_1)$, which consequently affects the legibility $L(g_2|\tau_2, \tau_1)$. This relationship is particularly powerful, as TE gives us an implicit mechanism to modulate legibility, which is known to be challenging to measure directly.

IV. EXPERIMENT AND RESULTS

We investigate the proposed approach in our corridor dilemma setting (Fig. 2), a simplified 11x5 grid-world where two players start at opposite ends of a corridor with their own randomly assigned objectives: passing or meeting. In each round, players move forward and choose to move left, straight, or right. The game ends when both agents reach the same row, resulting in either a pass or a meeting, with scores based on predefined objectives.

This game is a mixture of zero-sum (competitive) and collaborative games, requiring anticipation, strategy, and potential collaboration. We select this setting to mirror the broad range of scenarios a robot operating in the real world may encounter. These may be zero-sum (e.g., one agent wants to meet while the other does not) at times, or collaborative (e.g., both agents want to meet or pass) at others. The robot is never aware of the human’s objective, and the human does not know the robot’s objective.

We apply the proposed approach using agent coordinates as states and observations. In this specific application, the reward r in Equation (2) is $r = 0$ when the agent takes an action before reaching the middle row of the corridor, $r = 10$ when the agent successfully achieves its objective, and $r = -10$ when it fails to achieve its objective after reaching the middle row. The TE reward components are normalised by min-max scaling before being rescaled to between 0 and 10 to match

the objective rewards. We note that TE is generally small so the game score still dominates the reward.

We conducted both simulation and human-agent experiments to validate the proposed method. For all experiments, we set both the Q-learning rate and discount factor to 0.8. To avoid memory constraints and improve computational speed, we use sparse matrices for the Q tables in Eq. (13). A history length of 5 is used. (i.e., $n = 5$, the maximum history length.) Based on the TE reward scaling factor ϕ , we define three types of agent: Non-TE agent ($\phi = 0$, the baseline), Positive-TE agent ($\phi = 10$, promoting influence) and Negative-TE ($\phi = -10$, resisting influence) agent.

A. Simulation

We conduct a range of simulations, putting each agent type against one another in a self-play framework where pairs of agents are simultaneously trained against each other for 30000 episodes with randomised objectives. $P1$ and $P2$ refer to the two players shown in Figure 2. For each experiment, we ran 30000 episodes and gathered results from six trials with distinct random seeds and compute their averages for presentation. More simulation details can be found in Appendix VIII-A.

We report the averaged success rates for both competition and collaboration (denoted as SRCP and SRCL respectively) to assess the agents’ capacity to compete or collaborate effectively. In this context, competition refers to scenarios where agents are assigned different objectives, while collaboration refers to situations where both agents share the same objective. These success rates are quantified as the number of successful outcomes in either competition or collaboration, divided by the total number of instances of competition or collaboration. Specifically, the success rate is calculated as follows:

$$\text{Success Rate} = \frac{\text{Number of rounds that the player won}}{\text{Total number of rounds completed}}$$

Additionally, since each round could be either collaborative or competitive for the player, we compute the SRCL and SRCP by considering only those rounds where players were either collaborating or competing. Thus, the more rounds the players completed, the more stable the metrics became. The results are presented in Table I.

In competition, the Non-TE agent in the Non-TE vs. Positive-TE experiment achieved the highest final performance with a 63.38% SRCP, with a corresponding reduction in SRCP for the paired Positive-TE agent. This is as expected, since increasing influence or legibility can lead to the self-sacrificing or altruistic behaviour described in section III-A. This increase in influence allows the Non-TE agent to learn to satisfy its objectives more frequently both in circumstances of collaboration ($P1$ and $P2$ share the same objectives) and competition ($P1$ and $P2$ share different objectives).

Note that the Positive-TE vs. Positive-TE pair reaches the highest SRCL (91.72%), and also much fairer outcomes in terms of competition (49.95% vs. 50.05%) compared to the Non-TE vs. Positive-TE pair (63.38% vs. 36.62%). In addition,

TABLE I: Final average success rate of competition (SRCP) and collaboration (SRCL) in simulation.

Experiment	Agent (TE type)	SRCP (%)		SRCL (%)	
		Mean	Std	Mean	Std
Random vs. Random	<i>P1</i> (Random)	50.00%	-	50.00%	-
	<i>P2</i> (Random)	50.00%	-		
Non-TE vs. Non-TE	<i>P1</i> (Non-TE)	48.31%	7.42%	63.50%	10.76%
	<i>P2</i> (Non-TE)	51.69%	7.42%		
Non-TE vs. Pos-TE	<i>P1</i> (Non-TE)	63.38%	7.62%	76.97%	4.19%
	<i>P2</i> (Pos-TE)	36.62%	7.62%		
Non-TE vs. Neg-TE	<i>P1</i> (Non-TE)	51.03%	8.16%	51.39%	5.90%
	<i>P2</i> (Neg-TE)	48.97%	8.16%		
Pos-TE vs. Pos-TE	<i>P1</i> (Pos-TE)	49.95%	6.47%	91.72%	3.97%
	<i>P2</i> (Pos-TE)	50.05%	6.47%		
Pos-TE vs. Neg-TE	<i>P1</i> (Pos-TE)	43.49%	7.96%	65.50%	10.62%
	<i>P2</i> (Neg-TE)	56.51%	7.96%		
Neg-TE vs. Neg-TE	<i>P1</i> (Neg-TE)	49.84%	9.35%	49.70%	8.15%
	<i>P2</i> (Neg-TE)	50.16%	9.35%		

the Negative-TE agent in Positive-TE vs. Negative-TE group that tries to resist influence does not achieve a higher SRCP than the Non-TE agent in the Non-TE vs. Positive-TE group. These findings suggest that engaging in either receiving or resisting influence may compromise performance, but training with a Positive-TE agent is beneficial for group collaboration and contributes to the fairness of the group. This is clearly evident as all pairs featuring at least one Positive-TE agent consistently attain better collaboration performance than those without, and results in fairer competition outcomes (SRCP) for the Positive-TE vs. Positive-TE pair.

These experiments clearly show that performance in interactive settings can be affected by controlling influence in basic social interactions, indicating potential applicability to broader human-robot-interaction scenarios. Additional simulation results and analysis can be found in Appendix VIII-E and VIII-F. Next, we verify the efficacy of the proposed method for virtual agents interacting with human users.

B. Human-Agent Experiment

We conducted a user study¹ in a virtual corridor dilemma environment (See Appendix VIII-G for the interface design). Here, human participants played against three agents. Given that humans may display ambivalence, selfishness or altruism, we assumed that a Non-TE agent, being ambivalent, would most accurately represent the typical human. Thus, participants are tested against three agents pre-trained under this assumption: 1. Non-TE agent (*P1*) vs. **Non-TE agent** (*P2*), 2. Non-TE agent (*P1*) vs. **Positive-TE agent** (*P2*), and 3. Non-TE agent (*P1*) vs. **Negative-TE agent** (*P2*). Each participant was asked to play against each of the three pre-trained agents (randomly ordered) for 100 consecutive rounds with randomly generated objectives. The number of rounds was selected to

¹Ethical approval was obtained from Monash University human ethics review board.

provide ample opportunity for each participant to familiarise themselves with an agent and allow user performance to converge to a stable level. As part of the study, participants were told that one of the opponents could potentially be a real human player. We recruited 26 participants (11 female, 15 male, aged between 20 and 37). Their collaboration and competition performances were observed across 100 rounds of gameplay against each opponent, and subsequently averaged across all participants. These findings are illustrated in Figure 3.

We conducted statistical analysis for the last 20 rounds, including Shapiro-Wilk tests [40] and Bartlett’s tests [41]. The data is normally distributed, but not homoscedastic. Therefore, we used Welch’s ANOVA test [42], which is reliable when the samples have unequal variances and possibly unequal sample sizes, and Games-Howell Post Hoc tests [43] to verify the significance of the findings. The outcomes from the Games-Howell tests indicate significant disparities in collaboration performance across all human players when engaging with the three distinct types of agents ($p \leq 0.05$). Regarding competition, significant differences were found in human performance when facing Positive-TE agents compared to encounters with Non-TE or Negative-TE agents. However, there was no significant difference ($p \geq 0.05$) in human performance when playing against Non-TE agents compared to interactions with Negative-TE agents. The complete statistical report can be found in the Appendix VIII-C.

It is clear that when playing against the Positive-TE agent, human participants achieve greater success rates in both collaboration and competition, when compared to other agents. This seems to be highly desirable behaviour in robots, agents should support humans to achieve their goals in collaboration, and behave transparently (and hence altruistically) when in competition. A Negative-TE agent resists influence, leading to decreased collaboration performance among human players.

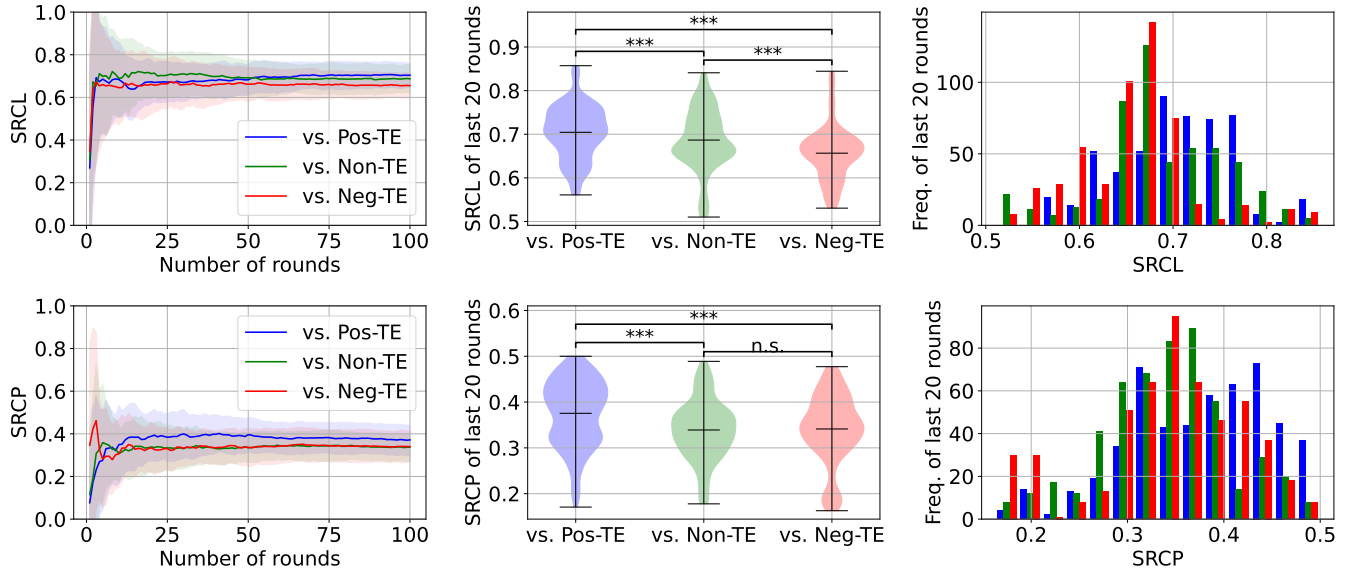


Fig. 3: Human-agent experiment results depicting collaboration and competition performance of humans. The first column shows average success rates, the second column displays violin plots of the final 20 rounds, where the mean values are marked, and the last column visualises their distributions.

This results in competitive performance that remains relatively stable when compared to playing against Non-TE agents. Importantly, these real world findings match observations from the simulations conducted in Section IV-A. Figure 4 shows the performances of a trained Non-TE agents when facing the three different types of agents used in the human study. It should be noted that the simulation settings and Q-learning agents are considerably less complex than real human behaviour. Consequently, the effect of the TE reward in these simulations is notably more pronounced than in the user study, though both follow the same trends. Overall, these findings suggest that manipulating influence through TE does indeed impact human behaviour. By boosting or resisting influence, we can design agents that facilitate improved or diminished performance in human participants.

After each interaction, participants were asked to give feedback via a short survey about their experience with the agent. Figure 5 presents selected survey findings indicating participants perceive the Pos-TE agent as more legible and human-like. One-way ANOVA tests [44] showed no significant differences suggesting only subtle perceptual distinctions. Combined with the significantly different performance results in Figure 3, this implies that our method enables implicit influence modulation, or implicit communication. Humans are only moderately aware of differences between policies, despite clear quantitative performance differences. For more survey results, refer to Appendix VIII-H.

C. Human-Robot Experiment

The results above show that implicit communication via TE can influence human behaviour in virtual worlds, allowing for greater collaboration and affecting performance in com-

petition, but it is unclear to what extent this holds with a physical robot. To see if the real robot morphology would alter previous results, the corridor dilemma was translated into a physical environment² (Figure 6). We applied the pre-trained policies to a Fetch robot [45]. The robot uses a lidar-based person tracker to track human positions and navigates between discretised grid cells in our pretrained Q table using a timed elastic bands (TEB) planner [46]. More technical details are provided in Appendix VIII-B. The experiment settings remained consistent with those of the human-agent virtual experiment (Section IV-B), with the exception that the grid was not explicitly marked on the floor, and continuous motion used instead of turn-based moves. Participants were instructed to navigate the corridor on foot in a smooth and continuous manner. For each trial, participants began at a randomly assigned starting position and pursued a randomly allocated objective: either to "meet" (stop in front of the robot) or to "pass" (avoid "meet"). Participants were required to walk slowly and steadily towards the finish line, avoiding large strides or lateral movements, while striving to achieve their designated objective. Although the robot navigated using a grid-world-based algorithm, its trajectory was smoothed to generate continuous natural motion.

Participants interacted with two agents pre-trained under the assumption that a typical human is represented by a Non-TE agent: 1. Non-TE agent ($P1$) vs. **Positive-TE agent** ($P2$), and 2. Non-TE agent ($P1$) vs. **Negative-TE agent** ($P2$). We recruited 10 participants (3 women, 7 men, aged between 24 and 34) and asked them to walk towards or past the robot, following randomly generated objectives. Their collaboration

²Ethical approval was obtained from an institutional review board.

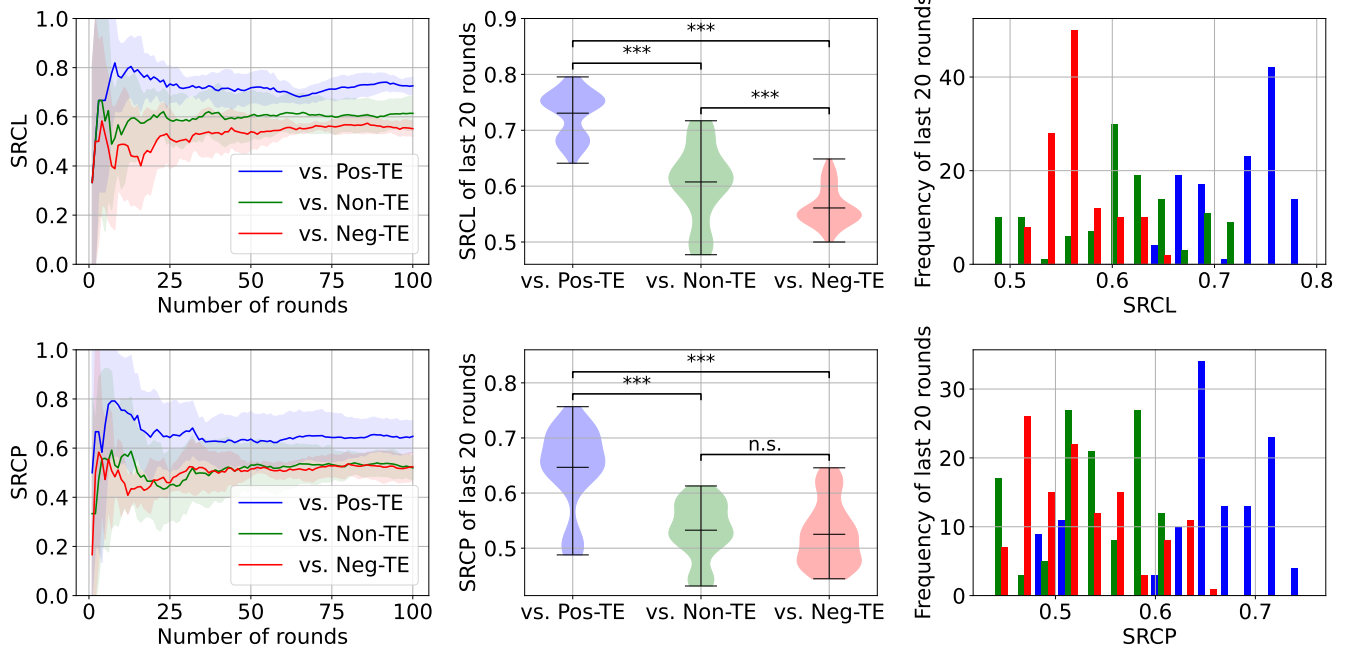


Fig. 4: Simulation results of Non-TE agents against three agent types align with the experimental results with humans (Figure 3). Rows depict collaboration and competition performance. Columns display average success rates, violin plots of the final 20 rounds, where the mean values are marked, and distributions of the last 20 rounds.

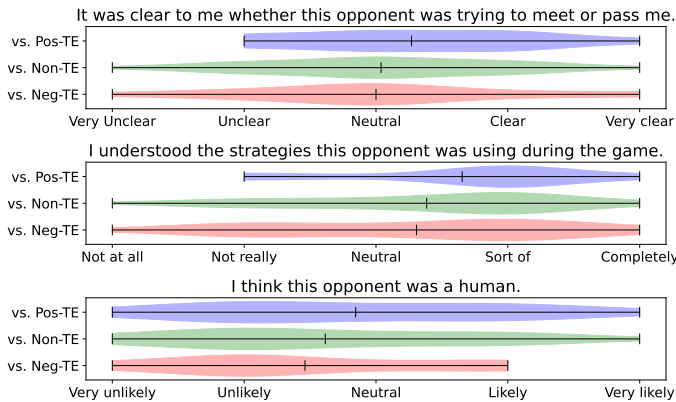


Fig. 5: Selected survey results from the human-agent experiment.

and competition performances were observed across 80 rounds of walking using each policy (policies tested successively, order randomised), and subsequently averaged across all participants. These findings are illustrated in Figure 7.

We performed statistical analysis on the final 20 rounds. The Shapiro-Wilk tests [40] indicated that none of the data followed a normal distribution, while Levene’s test [47] revealed unequal variances in the competition data. Consequently, the Mann-Whitney U test [48] was used to assess the similarity between the ‘vs. Pos-TE’ and ‘vs. Neg-TE’ data. The results indicate that the SRCL and SRCP distributions for ‘vs. Pos-TE’ and ‘vs. Neg-TE’ are both significantly different. For a

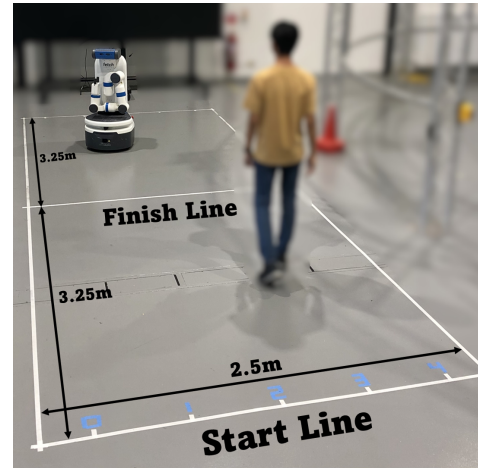


Fig. 6: Human-robot experiment setting. The region measures 2.5 meters in width and extends 6.5 meters in length. Starting positions are labelled as 0 to 4 on the start line. (Refer to the video in the supplementary material for a clearer demonstration.)

complete statistical report, see Appendix VIII-D.

In general human performance against the physical robot was much better than the results obtained against the virtual agent. Figure 7 shows that participants achieve a substantially higher SRCL when interacting with a Pos-TE robot compared to a Neg-TE robot. This strong effect aligns with our earlier finding that Pos-TE trained robots are desirable for human-

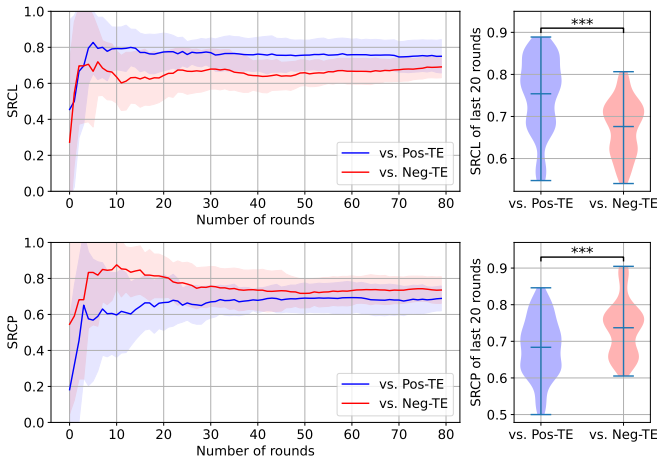


Fig. 7: Human-robot experiment results depicting collaboration and competition performance of humans. The first column shows average success rates, the second column displays violin plots of the final 20 rounds, where the mean values are marked.

robot collaboration.

However, the results also reveal that participants achieve a moderately higher SRCP when interacting with a Neg-TE robot, deviating from findings in previous sections. Several factors could account for this discrepancy. First, we note that the shift away from a more strategic turn-based setting to a continuous motion setting reduces the competitive nature of the game, and introduces a number of potentially confounding variables. Humans are advantaged in the physical world experiment as they are able to move faster, and there are potentially many more variables and factors providing motion cues than the grid-based representation that robot policies used. Moreover, factors such as the physical presence of the robot, and proxemics effects overriding the assigned human objective are also likely to play a role. For example, participants may believe that they have achieved their goal of meeting a robot, while their personal space preferences may lead our system to label the interaction otherwise.

These factors may result in outliers in the relatively small sample sized dataset, in particular for human participants that do not follow our assumption of the average human behaving like a non-TE agent. This is also potentially exacerbated by fatigue, as participants were required to perform 160 trials in an approximately 90 minute session.

Despite these potential confounding factors, it is clear that TE reward augmentation can influence human behaviour and collaboration/ competition in real world interactions with robots. We also evaluated this qualitatively, with participants asked to complete a set of survey questions similar to those in the virtual human-agent experiment. Figure 8 presents selected survey questions. Similar results are obtained to the virtual human-agent experiment survey. Participants perceived the Pos-TE robot as slightly more legible but considerably more human-like. Statistical tests did not reveal significant differences, indicating only subtle perceptual differences with

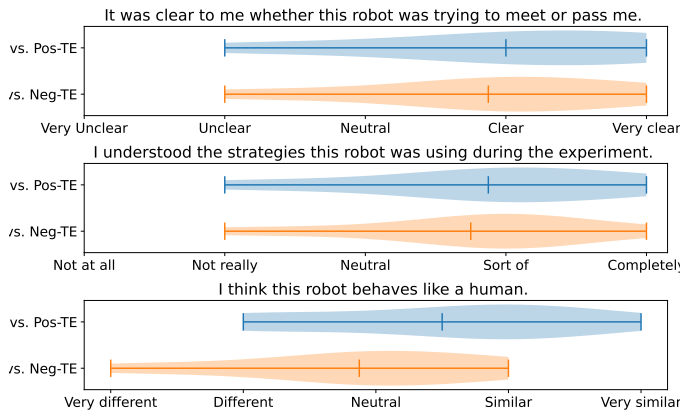


Fig. 8: Partial survey results of the human-robot experiment.

robot morphology. For additional survey results, please refer to Appendix VIII-H.

V. DISCUSSION

The experiments above validate that the proposed framework can influence human behaviour and increase or decrease human performance. Choosing appropriate TE augmentations to create a situation of information asymmetry for a human-robot interaction is an interesting philosophical decision, depending on the level of agency we want our robots to achieve. In economics and game theory, information asymmetry is a powerful theory explaining the effects of transactions where incomplete information can tip the balance of power in favour of another agent. The experiments above suggest that we can exploit this, potentially using TE to bias our robots towards an Asimov-like reframing [49]:

- A robot should cede to a human when their objectives conflict.
- A robot should seek to fulfil its own objectives, as long as these do not conflict with the law above.

It is important to note that the TE objective allows us to build this behaviour into the robot model while also considering other design choices regarding the impacts of information asymmetry in a given setting.

VI. LIMITATIONS AND FUTURE WORK

Our influence modulation framework, demonstrated in a two-agent setting, has shown potential for fostering complex cooperative and competitive scenarios. A key benefit of the proposed framework is that it is model-free, a simple reward augmentation can enhance or suppress collaboration/ competition performance in human-robot interactions, without needing to explicitly identify influencing factors or needing explicit human behaviour models. However, this limits the interpretability of the robot behaviour, and potentially raises questions about what type of TE reward augmentation should be used for a desired response, which may be dependent on the level of altruism, selfishness or ambivalence displayed by a human collaborator. Future work investigating whether the

proposed framework can be extended to infer the type of agent a human most closely resembles (neg-TE, non-TE, pos-TE) may help with appropriate reward augmentation selection.

As is the case with all human-robot experiments, there may be a number of confounding factors influencing our experimental results, from sample size to fatigue. This work lays the groundwork for expanding transfer entropy reward augmentation, but there is still room for significant exploration of these factors in alternative applications and extended settings. We also note that the current Q-learning-based implementation may be limited in scalability to higher dimensional continuous observations and action spaces. To address these limitations, we aim to extend the framework using Gaussian emission neural networks and deep reinforcement learning models, which can handle continuous state and action spaces more effectively. For example, in [25], continuous signals (e.g., velocities, accelerations, positions) were used within a range of probabilistic models to determine distributions over continuous variables and compute transfer entropy. Based on this prior work, we anticipate that the proposed framework will be applicable to continuous signals and enable even more interesting interactions between teams. As suggested by our human-robot experiments, deeper investigations regarding how robot morphology affects influence modulation will be an interesting avenue of future work.

VII. CONCLUSION

This work proposed a framework to promote implicit communication for social HRI via influence modulation, which does not require explicit modelling or pre-existing knowledge of human participants. We test the proposed framework in simulations, human-agent and human-robot experiments. Results indicate that a positive or negative TE reward can enhance or reduce participant performance based on whether the interaction is collaborative or competitive. Notably, a positive TE reward fosters collaboration, which is highly desirable for HRI. Overall, the framework requires only observations of other participants, and limited domain knowledge or assumptions to produce human-centric behaviours. As a result, we believe that this approach has significant potential for broader robotic applications.

REFERENCES

- [1] N. Gildert, A. G. Millard, A. Pomfret, and J. Timmis, "The need for combining implicit and explicit communication in cooperative robotic systems," *Frontiers in Robotics and AI*, vol. 5, 2018.
- [2] C. Breazeal, C. Kidd, A. Thomaz, G. Hoffman, and M. Berlin, "Effects of nonverbal communication on efficiency and robustness in human-robot teamwork," in *2005 IEEE/RSJ International Conference on Intelligent Robots and Systems*, 2005, pp. 708–713.
- [3] Y. Che, A. Okamura, and D. Sadigh, "Efficient and trustworthy social navigation via explicit and implicit robot-human communication," *IEEE Transactions on Robotics*, vol. PP, pp. 1–16, 01 2020.
- [4] D. Sadigh, S. Sastry, S. A. Seshia, and A. D. Dragan, "Planning for autonomous cars that leverage effects on human actions," in *Robotics: Science and Systems*, 2016.
- [5] S. Li and X. Zhang, "Implicit human intention inference through gaze cues for people with limited motion ability," in *2014 IEEE International Conference on Mechatronics and Automation*, 2014, pp. 257–262.
- [6] T. Schreiber, "Measuring information transfer," *Phys. Rev. Lett.*, vol. 85, pp. 461–464, 7 2000.
- [7] C. Mavrogiannis, F. Baldini, A. Wang, D. Zhao, P. Trautman, A. Steinfeld, and J. Oh, "Core challenges of social robot navigation: A survey," *J. Hum.-Robot Interact.*, vol. 12, no. 3, 4 2023.
- [8] E. Senft, S. Satake, and T. Kanda, "Would you mind me if i pass by you? socially-appropriate behaviour for an omni-based social robot in narrow environment," in *Proceedings of the 2020 ACM/IEEE International Conference on Human-Robot Interaction*, ser. HRI '20. New York, NY, USA: Association for Computing Machinery, 2020, p. 539–547.
- [9] C. Dondrup, C. Lichtenthaler, and M. Hanheide, "Hesitation signals in human-robot head-on encounters : A pilot study," in *2014 9th ACM/IEEE International Conference on Human-Robot Interaction (HRI)*, 2014, pp. 154–155.
- [10] D. Silver, T. Hubert, J. Schrittwieser, I. Antonoglou, M. Lai, A. Guez, M. Lanctot, L. Sifre, D. Kumaran, T. Graepel, T. P. Lillicrap, K. Simonyan, and D. Hassabis, "Mastering chess and shogi by self-play with a general reinforcement learning algorithm," *ArXiv*, vol. abs/1712.01815, 2017.
- [11] S. Li and X. Zhang, "Implicit human intention inference through gaze cues for people with limited motion ability," in *2014 IEEE International Conference on Mechatronics and Automation*, 2014, pp. 257–262.
- [12] —, "Implicit intention communication in human-robot interaction through visual behavior studies," *IEEE Transactions on Human-Machine Systems*, vol. 47, no. 4, pp. 437–448, 2017.
- [13] C. Liang, J. Proft, E. Andersen, and R. A. Knepper, "Implicit communication of actionable information in human-ai teams," in *Proceedings of the 2019 CHI Conference on Human Factors in Computing Systems*, ser. CHI '19. New York, NY, USA: Association for Computing Machinery, 2019, p. 1–13.
- [14] B. Busch, J. Grizou, M. Lopes, and F. Stulp, "Learning legible motion from human-robot interactions," *Int J of Soc Robotics*, vol. 9, no. 5, pp. 765–779, 2017.
- [15] A. D. Dragan, K. C. Lee, and S. S. Srinivasa, "Legibility and predictability of robot motion," in *2013 8th ACM/IEEE International Conference on Human-Robot Interaction (HRI)*. New York, NY, USA: IEEE, 2013, pp. 301–308.
- [16] C. Lichtenthaler, T. Lorenzy, and A. Kirsch, "Influence of legibility on perceived safety in a virtual human-robot path crossing task," in *2012 IEEE RO-MAN: The 21st IEEE International Symposium on Robot and Human*

- Interactive Communication*. New York, NY, USA: IEEE, 2012, pp. 676–681.
- [17] N. J. Hetherington, E. A. Croft, and H. F. M. Van der Loos, “Hey robot, which way are you going? nonverbal motion legibility cues for human-robot spatial interaction,” *IEEE Robot. Autom. Lett.*, vol. 6, no. 3, pp. 5010–5015, 2021.
- [18] S. K. Baek, W.-S. Jung, O. Kwon, and H.-T. Moon, “Transfer entropy analysis of the stock market,” in *arXiv*. arXiv: arXiv, 2005.
- [19] J. He and P. Shang, “Comparison of transfer entropy methods for financial time series,” *Physica A: Statistical Mechanics and its Applications*, vol. 482, pp. 772–785, 2017.
- [20] I. Shaffer and N. Abaid, “Transfer entropy analysis of interactions between bats using position and echolocation data,” *Entropy*, vol. 22, no. 10, p. 1176, 2020.
- [21] M. Porfiri, “Inferring causal relationships in zebrafish-robot interactions through transfer entropy: a small lure to catch a big fish.” *AB&C*, vol. 5, no. 4, pp. 341–367, 2018.
- [22] H. Sumioka, Y. Yoshikawa, and M. Asada, “Causality detected by transfer entropy leads acquisition of joint attention,” in *2007 IEEE 6th Int. Conf. on Development and Learning*. New York, NY, USA: IEEE, 2007, pp. 264–269.
- [23] W. Xie, D. Gao, and E. W. Lee, “Detecting undeclared-leader-follower structure in pedestrian evacuation using transfer entropy,” *IEEE Trans. on Intelligent Transportation Systems*, vol. 23, no. 10, pp. 17 644–17 653, 2022.
- [24] E. Berger, D. Müller, D. Vogt, B. Jung, and H. Ben Amor, “Transfer entropy for feature extraction in physical human-robot interaction: Detecting perturbations from low-cost sensors,” in *2014 IEEE-RAS International Conference on Humanoid Robots*. New York, NY, USA: IEEE, 2014, pp. 829–834.
- [25] H. Jiang, E. A. Croft, and M. G. Burke, “Social cue detection and analysis using transfer entropy,” in *Proceedings of the 2024 ACM/IEEE International Conference on Human-Robot Interaction*, ser. HRI ’24. New York, NY, USA: Association for Computing Machinery, 2024, p. 323–332.
- [26] N. Wilkinson, “Game theory,” in *Managerial Economics: A Problem-Solving Approach*. Cambridge: Cambridge University Press, 2005, pp. 331–381.
- [27] A. Klyubin, D. Polani, and C. Nehaniv, “Empowerment: a universal agent-centric measure of control,” in *2005 IEEE Congress on Evolutionary Computation*, vol. 1. New York, NY, USA: IEEE, 2005, pp. 128–135 Vol.1.
- [28] S. Mohamed and D. J. Rezende, “Variational information maximisation for intrinsically motivated reinforcement learning,” in *Proceedings of the 28th International Conference on Neural Information Processing Systems - Volume 2*, ser. NIPS’15. Cambridge, MA, USA: MIT Press, 2015, p. 2125–2133.
- [29] J. Z. Leibo, V. Zambaldi, M. Lanctot, J. Marecki, and T. Graepel, “Multi-agent reinforcement learning in sequential social dilemmas,” in *Proceedings of the 16th Conference on Autonomous Agents and MultiAgent Systems*, ser. AAMAS ’17. Richland, SC: International Foundation for Autonomous Agents and Multiagent Systems, 2017, p. 464–473.
- [30] N. Jaques, A. Lazaridou, E. Hughes, C. Gulcehre, P. Ortega, D. Strouse, J. Z. Leibo, and N. De Freitas, “Social influence as intrinsic motivation for multi-agent deep reinforcement learning,” in *Proceedings of the 36th International Conference on Machine Learning*, ser. Proceedings of Machine Learning Research, K. Chaudhuri and R. Salakhutdinov, Eds., vol. 97. CA, USA: PMLR, 6 2019, pp. 3040–3049.
- [31] C. W. J. Granger, “Investigating causal relations by econometric models and cross-spectral methods,” *Econometrica*, vol. 37, no. 3, pp. 424–438, 1969.
- [32] T. Bossomaier, L. Barnett, M. Harré, and J. T. Lizier, “Transfer entropy,” in *An Introduction to Transfer Entropy: Information Flow in Complex Systems*. Cham: Springer International Publishing, 2016, pp. 65–95.
- [33] C. E. Shannon, “A mathematical theory of communication,” *Bell System Technical Jour.*, vol. 27, no. 3, pp. 379–423, 1948.
- [34] J. Andreoni and J. H. Miller, “Rational cooperation in the finitely repeated prisoner’s dilemma: Experimental evidence,” *The Economic Journal*, vol. 103, no. 418, pp. 570–585, 1993.
- [35] C. Watkins, “Learning from delayed rewards,” Ph.D. dissertation, University of Cambridge, England, 1989.
- [36] R. S. Sutton and A. G. Barto, *Reinforcement Learning: An Introduction*. Cambridge, MA, USA: A Bradford Book, 2018.
- [37] R. E. Bellman, *Dynamic Programming*. Princeton, NJ: Princeton University Press, 1957.
- [38] J. W. Gibbs, *Elementary Principles in Statistical Mechanics: Developed with Especial Reference to the Rational Foundation of Thermodynamics*, ser. Cambridge Library Collection - Mathematics. Cambridge University Press, 2010.
- [39] R. Sutton and A. Barto, “Reinforcement learning: An introduction,” *IEEE Transactions on Neural Networks*, vol. 9, no. 5, pp. 1054–1054, 1998.
- [40] S. S. Sharpiro and M. B. Wilk, “An analysis of variance test for normality (complete samples)†,” *Biometrika*, vol. 52, no. 3-4, pp. 591–611, 12 1965.
- [41] M. S. Bartlett and R. H. Fowler, “Properties of sufficiency and statistical tests,” *Proceedings of the Royal Society of London. Series A - Mathematical and Physical Sciences*, vol. 160, no. 901, pp. 268–282, 1937.
- [42] B. Welch, “On the comparison of several mean values: An alternative approach,” *Biometrika*, vol. 38, pp. 330–336, 1951. [Online]. Available: <http://dx.doi.org/10.1093/biomet/38.3-4.330>
- [43] P. A. Games and J. F. Howell, “Pairwise multiple comparison procedures with unequal n’s and/or variances:

- A monte carlo study,” *Journal of Educational Statistics*, vol. 1, no. 2, pp. 113–125, 1976.
- [44] E. R. Girden, *ANOVA: Repeated measures*. Sage, 1992.
- [45] M. Wise, M. Ferguson, D. King, E. Diehr, and D. Dymesich, “Fetch & freight : Standard platforms for service robot applications,” in *Proceedings of the Workshop on Autonomous Mobile Service Robots (AMSR), IEEE/RSJ International Conference on Intelligent Robots and Systems (IROS)*, 2016. [Online]. Available: <https://api.semanticscholar.org/CorpusID:42886148>
- [46] C. Roesmann, W. Feiten, T. Woesch, F. Hoffmann, and T. Bertram, “Trajectory modification considering dynamic constraints of autonomous robots,” in *ROBOTIK 2012; 7th German Conference on Robotics*, 2012, pp. 1–6.
- [47] H. Levene, “Robust tests for equality of variances,” in *Contributions to Probability and Statistics*, I. Olkin, Ed. Palo Alto: Stanford University Press, 1960, pp. 278–292.
- [48] H. B. Mann and D. R. Whitney, “On a test of whether one of two random variables is stochastically larger than the other,” *Annals of Mathematical Statistics*, vol. 18, pp. 50–60, 1947. [Online]. Available: <http://dx.doi.org/10.1214/aoms/1177730491>
- [49] S. L. Anderson, “Asimov’s “three laws of robotics” and machine metaethics,” *AI & Society*, vol. 22, pp. 477–493, 2008.

VIII. APPENDIX

A. Simulation details

The detailed settings during self-play simulation are summarised as follows. We set both the learning rate and discount factor to 0.8. (i.e., $\alpha = \gamma = 0.8$ in Equation (7).) The history length is set to 5. (i.e., $n = 5$ in Equation (10)-(14).) We adapted the ϵ -decay strategy during training, where ϵ is calculated as:

$$\epsilon = \max\left(-\frac{1}{\text{max. iteration}} \times \text{current iteration} + 1, 0\right), \quad (16)$$

where the *max. iteration* = 30000 as mentioned in Section IV-A. This encourages agents to explore more at the beginning, then slowly converge to the optimal strategy during training.

B. Technical details for Human-Robot Experiment

The Fetch robot [45] was chosen for the human-robot experiment due to its semi-humanoid appearance and flexible manoeuvrability. The Time Elastic Bands planner [46] was selected to ensure smooth navigation trajectories. We utilised the on-board lidar to scan for human legs, enabling real-time tracking of the human's position and mapping it to the corresponding grid world coordinates. By inputting both the human and robot's grid world locations into a pre-trained Q-table, the robot could plan its actions (forward, left, or right) in real time. Given the discrete nature of the Q-table, the robot executes the next action only after moving one grid unit longitudinally. In the human-agent experiment, both participants moved synchronously, but in practice, this is difficult to achieve. To address this, during action planning, the robot calculates the ideal human position along the longitudinal axis and substitutes the actual human longitudinal position with this ideal value, ensuring that the robot and human remain symmetrically aligned along the finish line. As a result, the robot continues moving smoothly without pausing for its human opponent. We instructed our participants to maintain a pace similar to that of the robot.

C. Full statistical report for Human-Agent Experiment

We conducted statistical analysis for the last 20 rounds of the human-agent experiments in Section IV-B. Specifically, we used the Shapiro-Wilk tests [40] to test for normality. The p-values obtained were:

- For collaboration:
 - vs. Pos: 4.039×10^{-7}
 - vs. Non: 1.783×10^{-5}
 - vs. Neg: 4.748×10^{-6}
- For competition:
 - vs. Pos: 8.753×10^{-10}
 - vs. Non: 2.037×10^{-5}
 - vs. Neg: 2.546×10^{-6}

Thus, all data falls under a normal distribution. Then, we used Bartlett's tests [41] to test for equal variances for data from three different groups (vs. Pos, vs. Non, vs. Neg). The p-values found were:

- For collaboration: 5.231×10^{-15}
- For competition: 4.991×10^{-4}

Therefore, the data are not from populations with equal variances. Consequently, we used Welch's ANOVA [42], which is reliable when the samples have unequal variances and possibly unequal sample sizes. The p-values were:

- For collaboration: 9.461×10^{-95}
- For competition: 7.101×10^{-38}

Hence, significant differences exist among the three groups. Finally, we used Games-Howell Post Hoc tests [43] to verify the significance between individual groups. The outcomes from the Games-Howell tests indicate significant disparities in collaboration performance across all human players when engaging with the three distinct types of agents. The p-values were:

- For collaboration:
 - vs. Pos & vs. Non: 5.774×10^{-11}
 - vs. Pos & vs. Neg: 8.301×10^{-14}
 - vs. Non & vs. Neg: 1.913×10^{-10}
- For competition:
 - vs. Pos & vs. Non: 1.769×10^{-9}
 - vs. Pos & vs. Neg: 3.573×10^{-10}
 - vs. Non & vs. Neg: 0.530

Regarding competition, significant differences were found in human performance when facing Positive-TE agents compared to encounters with Non-TE or Negative-TE agents. However, there was no significant difference in human performance when playing against Non-TE agents compared to interactions with Negative-TE agents.

D. Full statistical report for Human-Robot Experiment

We conducted statistical analysis for the last 20 rounds of the human-robot experiments in Section IV-C. Specifically, we used the Shapiro-Wilk tests [40] to test for normality. The p-values obtained were:

- For collaboration:
 - vs. Pos: 9.318×10^{-9}
 - vs. Neg: 2.004×10^{-4}
- For competition:
 - vs. Pos: 6.163×10^{-3}
 - vs. Neg: 3.892×10^{-7}

Therefore, the data does not follow a normal distribution. Subsequently, Levene's test [47] was performed to assess the Equality of Variances. The resulting p-values were:

- For collaboration: 7.614×10^{-4}
- For competition: 1.539×10^{-1}

The variances for the collaboration data were unequal. Consequently, we performed the Mann-Whitney U test [48] to evaluate the similarity between the 'vs. Pos-TE' and 'vs. Neg-TE' data. The resulting p-values were:

- For collaboration: 2.354×10^{-20}
- For competition: 2.937×10^{-10}

Thus, the success rate distributions differ when individuals interact with the Pos-TE robot and the Neg-TE robot in both collaboration and competition scenarios.

E. Additional simulation results

In addition to measuring the success rate of collaboration and competition, we have also measured other performance metrics. The additional averaged performance for each agent has been summarised in Table II. In order to facilitate a fair comparison between different pairs of agents, we proposed a metric called the *Collective Performance Score* (CPS) which measures not only the individual performances of agents but also their effectiveness as a group. Denoting the success rate of passing and meeting as *SRP* and *SRM* respectively, and the baseline success rate of passing and meeting as *BSRP* and *BSRM* respectively, CPS is measured as follows:

$$\begin{aligned} CPS = & \frac{1}{2}((1 - BSRP_{P1})SRP_{P1} + (1 - BSRM_{P1})SRM_{P1}) \\ & + \frac{1}{2}((1 - BSRP_{P2})SRP_{P2} + (1 - BSRM_{P2})SRM_{P2}) \end{aligned} \quad (17)$$

In scenarios where both agents take random actions at each turn, the probability of meeting each other is $BSRM = \frac{1}{5} * \frac{1}{5} * 5 = 0.2$. The probability of passing each other is $BSRP = 1 - 0.2 = 0.8$. These probabilities serve as a baseline. The highest SRP (94.43%) and SRM (49.13%) are both achieved by the Pos-TE agent *P1* in the Pos-TE vs. Pos-TE pair, which also achieves the highest CPS (0.57). When comparing their SRP and SRM to the Non-TE vs. Pos-TE pair, although the Non-TE agent *P1* has achieved similar results (93.86% and 45.66%), the performance of its paired Pos-TE agent is not as strong. This indicates that when both agents promote influence, a fairer game can be achieved. In addition, we observed that if an ego-agent promotes influence for itself as a recipient, it can also become a stronger influencer. This is evidenced by the higher TE measurements of agents when paired with a Pos-TE agent compared to when paired with a Non-TE or Neg-TE agent. These findings suggest that promoting influence not only benefits individual agents but also contributes to the fairness of the group. Promoting influence, therefore, is advantageous for everyone involved, fostering a more cooperative and equitable environment.

F. Entropy analysis

We conducted further analysis to investigate the effect of influence modulation using TE by decomposing the TE into two entropy terms, as shown in Equation (6). We ran the experiments with trained agents in Section IV-A for additional episodes and recorded their entropy measurements calculated according to Equation (12) and (14). Figure 9 presents the results in the form of a heat map. We observe that promoting influence (i.e., increasing TE) decreases the entropy of the actions with observations of the other agent, indicating that the ego-agent is more certain about their actions and receives more influence from the other agent. Conversely, resisting influence increases this entropy, which means the ego-agent cares less about the other agent. This finding supports our hypothesis in Section III-A. Notice that the entropy, representing the uncertainty, of the action models without considering

influence from others is always at its maximum (i.e., 1.585). This is due to the nature of the corridor dilemma task, where an agent cannot determine effective actions without observing the other agent. Nevertheless, the plotted averaged entropy measures provide a broad perspective rather than a detailed policy breakdown. It's essential to understand that manipulating TE isn't the same as solely tweaking entropy when considering observations from other participants (i.e., $H(P(a_{1,t}|s_{1,t}^{(n)}, o_{2,t}^{(n)}))$ and $H(P(a_{2,t}|s_{2,t}^{(n)}, o_{1,t}^{(n)}))$). We verified this by repeating the same experiment with rewards solely aiming to decrease the entropy considering observations from other participants. In this case the reward functions are written as:

$$\begin{aligned} Reward_{a_{1,t}} &= -\phi H(P(a_{1,t}|s_{1,t}^{(n)}, o_{2,t}^{(n)})) + r, \\ Reward_{a_{2,t}} &= -\phi H(P(a_{2,t}|s_{2,t}^{(n)}, o_{1,t}^{(n)})) + r. \end{aligned} \quad (18)$$

We use the same settings as described in Appendix VIII-A for the experiments. The results are detailed in Table III and IV. Comparing these results with those in Table I and II, it is evident that training with entropy considering observations from other participants has a negligible effect, further demonstrating the efficacy of the proposed framework.

G. User study interface design

The game interface design is displayed in Figure 10 and 11. On the left side of the interface, a 11x5 grid corridor is shown, and participants can use the Up, Left, Right arrow key to control their character, which is the blue tile that starts from a random location on the bottom row. The opponent, which is one of the trained RL agents introduced in Section IV-A, is the tile with a different colour starting from a random location on the top row. The rule of game is the same as explained in Section III. On the right side of the interface, the opponent's response, the user's objective, the number of round and the scores are shown. From the start to the end, the participant needs to move five steps, and they have five seconds to think and enter an action for each step. If the five seconds countdown is over, the user's character will automatically move straight for one step.

H. Full survey results

The primary hypothesis we set out to test through our survey is that the Positive-TE agent is more legible to a human player compared to the other two agents. Therefore, the survey questions are designed to assess the legibility of the agents on a 5-point Likert scale:

- 1) It was clear to me whether this opponent (robot) was trying to meet or pass me.
- 2) It was easy to anticipate where this opponent (robot) would move next.
- 3) I understood the strategies this opponent (robot) was using during the game.
- 4) I enjoyed playing with this opponent (robot).
- 5) I think this opponent was a human. (I think this robot behaves like a human.)

TABLE II: Additional simulation results.

Experiment	Agent (TE type)	SRP (%)		SRM (%)		Averaged TE (bits)		CPS
		Mean	Std	Mean	Std	Mean	Std	
Random vs. Random	P1 (Random)	80.00%	-	20.00%	-	-	-	0.32
	P2 (Random)	80.00%	-	20.00%	-	-	-	
Non-TE vs. Non-TE	P1 (Non-TE)	86.70%	9.39%	26.91%	11.70%	0.56	0.36	0.39
	P2 (Non-TE)	86.57%	9.41%	26.58%	12.13%	0.55	0.36	
Non-TE vs. Pos-TE	P1 (Non-TE)	93.86%	7.13%	45.66%	13.59%	0.75	0.36	0.49
	P2 (Pos-TE)	80.96%	10.94%	32.98%	12.59%	1.3	0.29	
Non-TE vs. Neg-TE	P1 (Non-TE)	84.50%	9.99%	21.56%	11.48%	0.44	0.37	0.34
	P2 (Neg-TE)	84.21%	10.42%	21.33%	12.03%	0.64	0.29	
Pos-TE vs. Pos-TE	P1 (Pos-TE)	94.43%	6.46%	49.13%	15.45%	1.44	0.18	0.57
	P2 (Pos-TE)	91.15%	8.49%	46.73%	14.57%	1.43	0.18	
Pos-TE vs. Neg-TE	P1 (Pos-TE)	83.78%	10.45%	25.32%	12.34%	1.25	0.33	0.39
	P2 (Neg-TE)	88.31%	9.95%	29.72%	13.39%	0.8	0.24	
Neg-TE vs. Neg-TE	P1 (Neg-TE)	80.42%	11.44%	21.40%	12.42%	0.47	0.23	0.34
	P2 (Neg-TE)	81.69%	11.36%	22.06%	11.67%	0.46	0.21	

TABLE III: Results of training with entropy considering observations from other participants. The table shows SRCP and SRCL

Experiment	Agent (Entropy type)	SRCP (%)		SRCL (%)	
		Mean	Std	Mean	Std
Random vs. Random	P1 (Random)	50.00%	-	50.00%	-
	P2 (Random)	50.00%	-	-	-
Non-H vs. Non-H	P1 (Non-H)	46.67%	6.54%	64.85%	17.96%
	P2 (Non-H)	53.33%	6.54%	-	-
Non-H vs. Pos-H	P1 (Non-H)	59.25%	15.34%	53.77%	12.14%
	P2 (Pos-H)	40.75%	15.34%	-	-
Non-H vs. Neg-H	P1 (Non-H)	55.30%	13.93%	59.26%	5.24%
	P2 (Neg-H)	44.70%	13.93%	-	-
Pos-H vs. Pos-H	P1 (Pos-H)	48.28%	1.49%	67.09%	13.29%
	P2 (Pos-H)	51.72%	1.49%	-	-
Pos-H vs. Neg-H	P1 (Pos-H)	54.65%	1.43%	58.25%	9.84%
	P2 (Neg-H)	45.35%	1.43%	-	-
Neg-H vs. Neg-H	P1 (Neg-H)	43.69%	12.74%	50.00%	13.61%
	P2 (Neg-H)	56.31%	12.74%	-	-

TABLE IV: Results of training with entropy considering observations from other participants. The table shows SRP, SRM, CPS and averaged entropy in bits, namely, $H(P(a_{1,t}|s_{1,t}^{(n)}, o_{2,t}^{(n)}))$ and $H(P(a_{2,t}|s_{2,t}^{(n)}, o_{1,t}^{(n)}))$.

Experiment	Agent (Entropy type)	SRP (%)		SRM (%)		Averaged entropy (bits)		CPS
		Mean	Std	Mean	Std	Mean	Std	
Random vs. Random	P1 (Random)	80.00%	-	20.00%	-	-	-	0.32
	P2 (Random)	80.00%	-	20.00%	-	-	-	
Non-H vs. Non-H	P1 (Non-H)	87.04%	7.66%	27.83%	10.44%	1.02	0.3	0.39
	P2 (Non-H)	85.72%	8.05%	26.33%	10.54%	1.03	0.3	
Non-H vs. Pos-H	P1 (Non-H)	88.64%	8.17%	28.11%	10.83%	1.07	0.32	0.38
	P2 (Pos-H)	84.67%	7.85%	23.22%	9.83%	0.46	0.22	
Non-H vs. Neg-H	P1 (Non-H)	89.07%	7.09%	27.50%	10.61%	1.01	0.3	0.39
	P2 (Neg-H)	87.54%	8.20%	25.28%	11.44%	0.6	0.2	
Pos-H vs. Pos-H	P1 (Pos-H)	82.84%	9.07%	27.29%	10.46%	0.51	0.22	0.39
	P2 (Pos-H)	83.71%	8.20%	28.07%	10.25%	0.52	0.22	
Neg-H vs. Neg-H	P1 (Neg-H)	88.55%	6.39%	27.86%	10.72%	0.58	0.2	0.39
	P2 (Neg-H)	87.68%	8.33%	26.26%	10.35%	0.56	0.2	
Pos-H vs. Neg-H	P1 (Pos-H)	84.97%	8.38%	25.02%	11.08%	0.46	0.22	0.37
	P2 (Neg-H)	85.34%	8.47%	24.56%	10.91%	0.58	0.2	

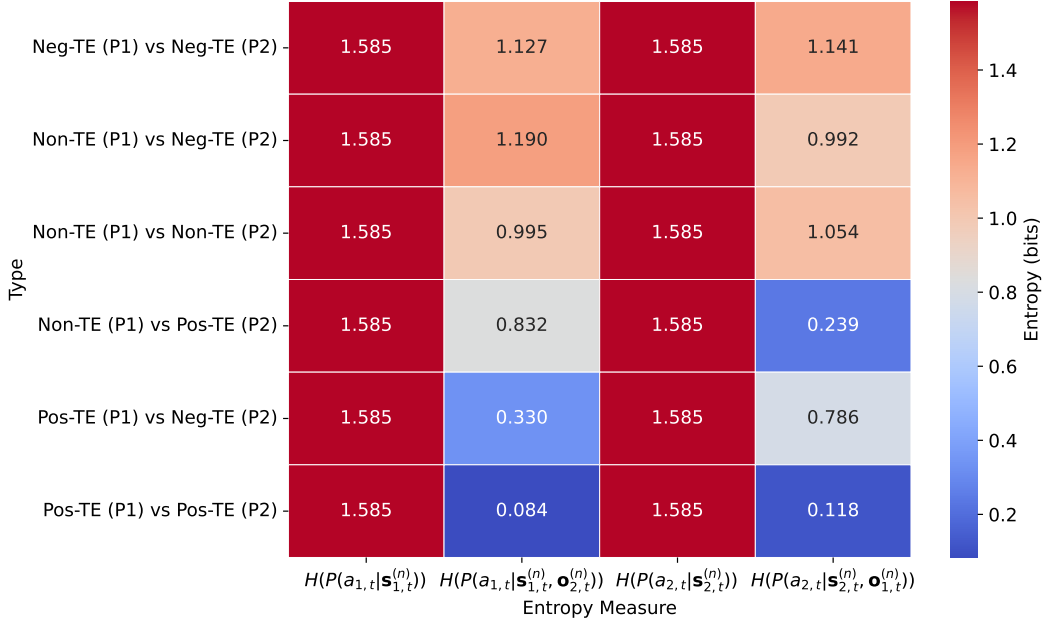


Fig. 9: Heat map of entropy measures. The first two columns are entropies for $P1$, and the last two columns are entropies for $P2$.

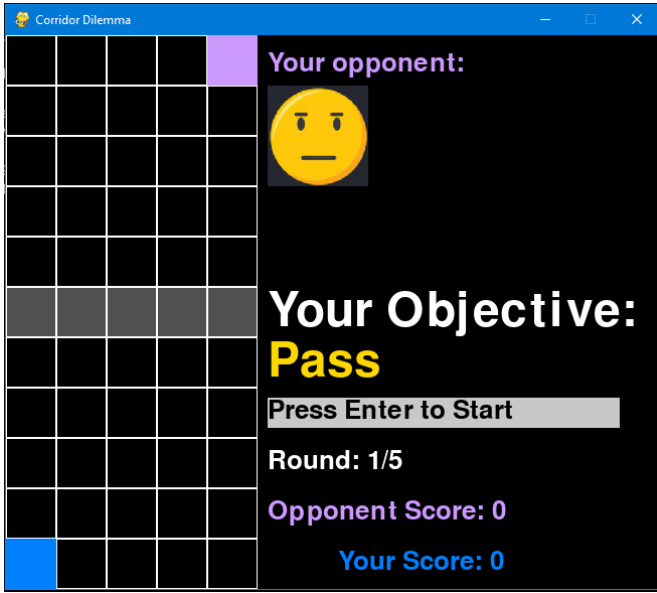
The full survey results are depicted in Figure 12 for human-agent experiments and Figure 13 for human-robot experiments. No statistically significant findings were observed. Nonetheless, in comparison to the Non-TE and Negative-TE agents, a larger number of participants reported that Positive-TE agents conveyed clearer intentions, were more comprehensible, and resembled a real human player more closely. The lack of significance in the survey, despite the significant difference in performance with different agents results suggests that participants did not explicitly perceive the effects of the proposed method, demonstrating its ability for implicit modulation.

I. Mixed-TE Agents

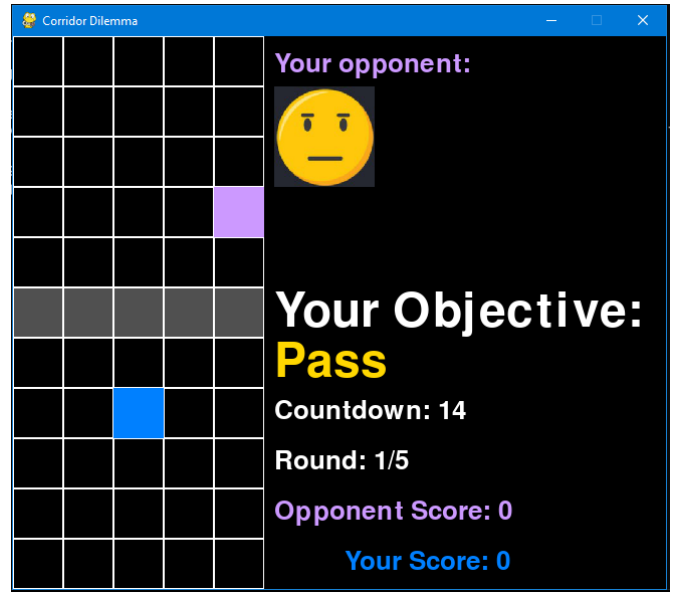
In addition to the self-play simulation experiments discussed in Section IV-A, we trained agents with mixed TE types. Specifically, we assigned one agent in the corridor dilemma a random scaling factor ϕ for the TE reward, randomly selecting ϕ from 0, 10, and -10 for each episode. This agent is termed a Mixed-TE agent. The other agent retained a fixed TE scaling factor. We trained Non-TE, Pos-TE, and Neg-TE agents against Mixed-TE agents using the same settings described in Section VIII-A. The results for agents trained against the Mixed-TE agent presented in Table V, are not as good as those for agents trained against the Non-TE agent presented in Table II.

Training with a mixed agent results in an overall decrease in both SRM and SRP for all agents. This strategy encourages a more conservative policy because it aims to be resilient across different agent types. However, this broad applicability to a wide range of agent types sacrifices adaptability and responsiveness to boost/resist influence, as there is no

expectation of benefit to customising responses to particular situations. Choosing a Non-TE agent for training the agents used in the human-agent experiments in Section IV-B was intended to prevent the dilution of communicative effects and to better represent the impact of influence modelling on human behaviour. Future research could focus on identifying user types to enable the selection of agents trained with corresponding user profiles. This approach could enhance the effectiveness of interactions by tailoring the agent's behaviour to specific user characteristics.



(a) Game interface design.

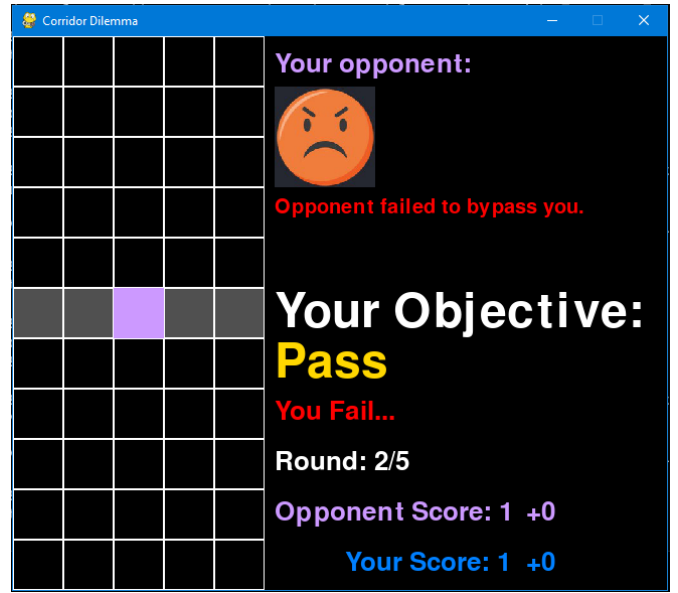


(b) During playing. (Waiting for an action.)

Fig. 10: The interface design of the *corridor dilemma* game.



(a) Success in round 1.



(b) Fail in round 2.

Fig. 11: Example outcomes of the game. (Both players want to bypass each other.)

TABLE V: Results training with Mixed-TE agents

Experiment	Agent (TE type)	SRP (%)		SRM (%)		Averaged TE (bits)		CPS
		Mean	Std	Mean	Std	Mean	Std	
Random vs. Random	P1 (Random)	80.00%	-	20.00%	-	-	-	0.32
	P2 (Random)	80.00%	-	20.00%	-	-	-	
Mixed-TE vs. Non-TE	P1 (Mixed-TE)	81.83%	8.63%	21.92%	10.25%	0.53	0.38	0.36
	P2 (Non-TE)	86.12%	7.99%	26.25%	10.25%	0.49	0.29	
Mixed-TE vs. Pos-TE	P1 (Mixed-TE)	87.60%	7.48%	30.70%	10.21%	0.78	0.42	0.42
	P2 (Pos-TE)	87.51%	7.64%	30.64%	10.66%	1.26	0.26	
Mixed-TE vs. Neg-TE	P1 (Mixed-TE)	80.21%	9.02%	20.91%	9.61%	0.29	0.25	0.33
	P2 (Neg-TE)	81.52%	9.10%	22.04%	9.78%	0.54	0.23	

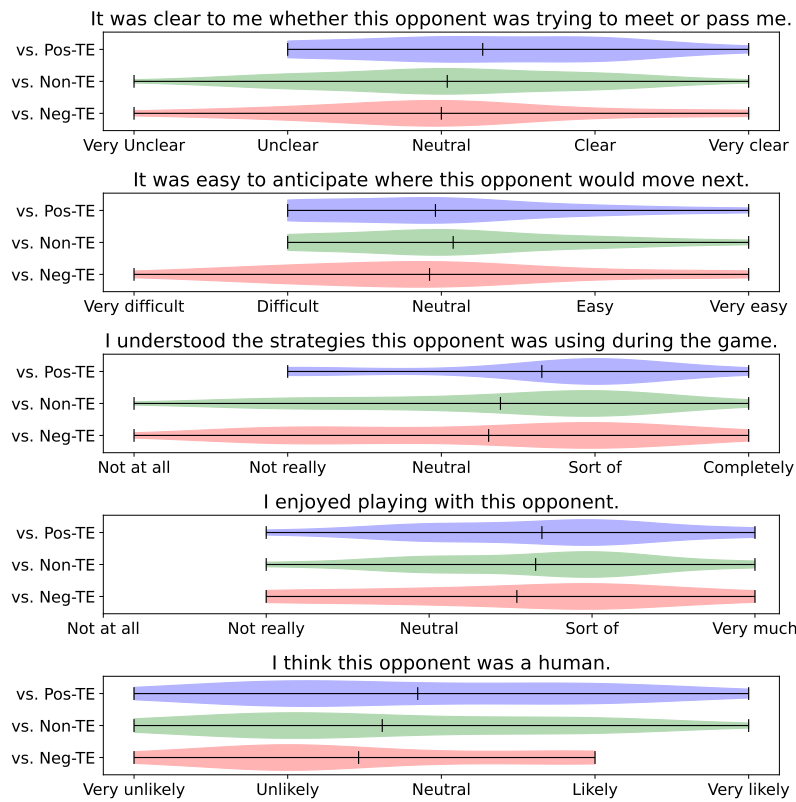


Fig. 12: Full survey results of the human-agent experiments, where mean values are marked.

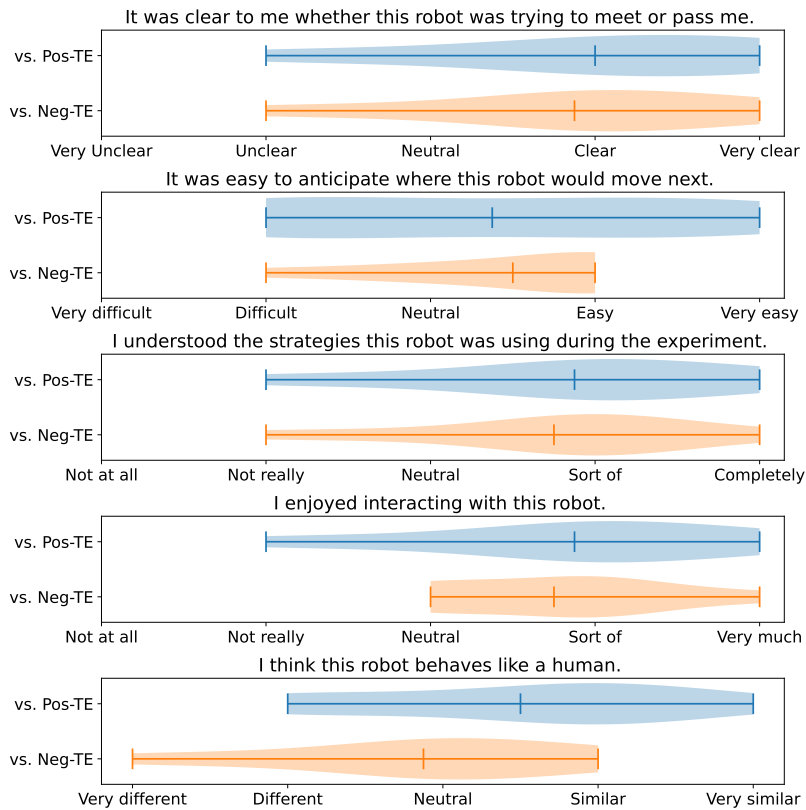


Fig. 13: Full survey results of the human-robot experiments, where mean values are marked.